*The American Journal of Pathology, Vol. 173, No. 3, September 2008*

*DOI: 10.2353/ajpath.2008.071176*

*Cell Injury, Repair, Aging and Apoptosis*

# Neuronal Apoptosis and Autophagy Cross Talk in Aging PS/APP Mice, a Model of Alzheimer's Disease

Dun-Sheng Yang,*† Asok Kumar,*† Philip Stavrides,* Jesse Peterson,‡ Corrine M. Peterhoff,* Monika Pawlik,*§ Efrat Levy,*†§ Anne M. Cataldo,‡ and Ralph A. Nixon*†¶

*From the Center for Dementia Research,* Nathan S. Kline Institute, Orangeburg, New York; the Departments of Psychiatry,† Cell Biology,¶ and Pharmacology,§ New York University School of Medicine, New York, New York; and the Mailman Research Center,‡ McLean Hospital, Harvard University, Belmont, Massachusetts*

**Mechanisms of neuronal loss in Alzheimer's disease (AD) are poorly understood. Here we show that apoptosis is a major form of neuronal cell death in PS/APP mice modeling AD-like neurodegeneration. Pyknotic neurons in adult PS/APP mice exhibited apoptotic changes, including DNA fragmentation, caspase-3 activation, and caspase-cleaved α-spectrin generation, identical to developmental neuronal apoptosis in wild-type mice. Ultrastructural examination using immunogold cytochemistry confirmed that activated caspase-3-positive neurons also exhibited chromatin margination and condensation, chromatin balls, and nuclear membrane fragmentation. Numbers of apoptotic profiles in both cortex and hippocampus of PS/APP mice compared with age-matched controls were twofold to threefold higher at 6 months of age and eightfold higher at 21 to 26 months of age. Additional neurons undergoing dark cell degeneration exhibited none of these apoptotic features. Activated caspase-3 and caspase-3-cleaved spectrin were abundant in autophagic vacuoles, accumulating in dystrophic neurites of PS/APP mice similar to AD brains. Administration of the cysteine protease inhibitor, leupeptin, promoted accumulation of autophagic vacuoles containing activated caspase-3 in axons of PS/APP mice and, to a lesser extent, in those of wild-type mice, implying that this pro-apoptotic factor is degraded by autophagy. Leupeptin-induced autophagic impairment increased the number of apoptotic neurons in PS/APP mice. Our findings establish apoptosis as a mode of neuronal cell death in aging PS/APP mice and identify the cross talk between autophagy and apoptosis, which influences neuronal survival in AD-related neurodegeneration.** ***(Am J Pathol 2008, 173:665–681; DOI: 10.2353/ajpath.2008.071176)***

Alzheimer's disease (AD) is associated with the widespread loss of neurons, which correlates with the severity of clinical symptoms.[1–4] Little is known, however, about the molecular mechanisms that mediate neuronal cell death in AD. Complicating this analysis are observations that multiple proteolytic systems are activated as neurons slowly degenerate in AD brain, including calpains,[5,6] the lysosomal system (cathepsins),[7] and caspases.[8,9] Apoptosis, a highly regulated process of cell death, is often proposed as a possible mode of neuronal death in AD[10] based on the presence in affected neurons of fragmented DNA detected by the terminal deoxynucleotidyl transferase-mediated dUTP nick-end labeling (TUNEL),[11–15] activated caspases,[16–20] and products of caspase-specific protein cleavage.[21–26]

Apoptosis is characterized morphologically by cytoplasmic shrinkage, chromatin condensation, nuclear and cellular fragmentation, and the formation of apoptotic bodies. Typical nuclear changes include highly compact chromatin masses with geometrically regular shapes. Cell membrane integrity and mitochondria are primarily unchanged morphologically in the early stage. The period from initiation to execution of apoptosis has been estimated to be hours or days, and apoptotic bodies are rapidly phagocytosed by adjacent cells or macrophages. Therefore, at a single moment in time in a chronic neurodegenerative disease, only a few cells that are undergoing apoptosis can be detected.[10,27–33] Ultrastructural features of *in vivo* neuronal apoptosis in mammalian brains have been recently described in detail by Dikranian and colleagues[34] including formation of condensed

Supported by the National Institute on Aging (grant P01 AG017617 to R.A.N.) and the Alzheimer's Association (to R.A.N.).

Accepted for publication June 12, 2008.

Supplemental material for this article can be found on *http://ajp.amjpathol.org.*

Address reprint requests to Dun-Sheng Yang, Ph.D., Nathan Kline Institute, New York University School of Medicine, 140 Old Orangeburg Rd., Bldg. 39, Orangeburg, NY 10962. E-mail: dyang@nki.rfmh.org.

chromatin balls (CBs) and apoptotic bodies, fragmentation of nuclear membranes, disassociation of the nucleolus, and either intact cytoplasmic organelles or transformation of cytoplasmic contents into nondescript particulate or membranous debris, depending on the stages in the apoptotic process. Activation of the caspase cascade is the most central and pathognomonic biochemical event in apoptosis. Various stimuli trigger the death receptor, the mitochondrial or the endoplasmic reticulum stress pathway to activate initiator caspases such as caspase-8, -9, or -12, which, in turn, activate effector caspases including caspases-3, -6, and -7. Activated effector caspases cleave various vital cellular substrates including structural proteins such as lamin, actin, and spectrin resulting in characteristic features of apoptotic morphology.[35–39] DNA fragmentation—cleavage of chromosomal DNA into mono- and oligonucleosome-sized fragments—is another biochemical hallmark in apoptosis[40] that can be detected biochemically by agarose gel electrophoresis[41] or morphologically by the incorporation of labeled dUTP by the TUNEL method.[42]

A possible opposing influence on apoptosis is autophagy,[43–45] a major lysosomal pathway for the turnover of organelles and cytoplasmic constituents, including pathological protein aggregates.[46–50] During states of nutritional deprivation or trophic factor withdrawal, autophagy delays or prevents apoptosis by turning over nonessential cell constituents to provide substrates for energy.[51] Autophagy induction in injury states eliminates damaged organelles that could trigger cell death. Autophagy is, therefore, commonly considered a cytoprotective response, which can become permissive or facilitative for apoptosis or necrosis if autophagy fails in pathological states.[44,45] In certain conditions, overactivated autophagy can also initiate an autophagic pattern of programmed cell death distinct from apoptosis.[52–54] Autophagy is induced but impaired in affected neurons in AD brain[55,56] causing autophagic vacuoles (AVs) to accumulate profusely in dystrophic neurites. The relationship of autophagy to neuronal survival or death, however, remains unclear.

Neuron loss is limited in most mouse models of $\beta$-amyloidosis, although it is significant in some animal models, particularly those expressing mutations in two AD-related genes. In PS/APP mice[57] that express mutant human presenilin 1 *(PS)* and mutant amyloid precursor protein *(APP)*, $\beta$-amyloid is deposited progressively in the brain beginning at 8 weeks of age,[58] and is associated with the extensive dystrophy of neurites containing marked accumulations of AVs.[56,58] Stereological analyses have demonstrated significant hippocampal neuronal cell loss in PS/APP mice at 22 months of age,[59] which have not been seen in young adult PS/APP mice[60]; however, molecular events involved in the compromise and loss of these cells are unexplained.

Here we investigated apoptosis as a possible basis for neuronal cell death in the PS/APP mouse using, for the first time, concurrent morphological and biochemical criteria for apoptosis validated in the well-established model of programmed neuronal cell death that occurs in early postnatal mouse brain development. This combined approach demonstrated unequivocal apoptosis of neurons in the PS/APP cortex and hippocampus and provided evidence for cross talk between apoptosis and autophagy in the neurodegenerative process.

## Materials and Methods

### Animals

All procedures were performed following the National Institutes of Health Guidelines for the Humane Treatment of Animals, with approval from the Institutional Animal Care and Use Committee at the Nathan Kline Institute. Animals of both sexes were used in this study. The transgenic PS/APP mice, which expressed both the Swedish double mutations of *APP* (K670N/M671L) and mutant *PS1* (PS1M146L), were generated as previously described.[57] An equal number of age-matched wild-type (WT) mice were used as controls. Additional neonatal mouse brains were obtained from normal C57BL/6J mice on postnatal day 5. All of the animals were anesthetized with a mixture (0.01 ml/g body weight, i.p.) of ketamine (10 mg/ml) and xylazine (1 mg/ml) and fixed by perfusion with aldehydes.

### Immunocytochemistry

PS/APP and WT mice ($n = 4$ for each of 6 months old or 16 months old of each genotype; $n = 8$ for 21 to 26 months old of each genotype) or neonatal C57BL/6J mice ($n = 5$) were fixed by cardiac perfusion using 4% paraformaldehyde in 0.1 mol/L sodium cacodylate buffer. After perfusion fixation, the brains were immersion-fixed in the same fixative overnight at 4°C. Forty-$\mu$m-thick vibratome sections were cut and processed for immunocytochemistry using the following primary antibodies: polyclonal anti-activated caspase-3 (catalog no. 9661; Cell Signaling, Beverly, MA), rabbit antibody Ab246 (recognizing caspase-cleaved $\alpha$-spectrin fragments, a kind gift from Dr. Robert Siman, University of Pennsylvania, Philadelphia, PA),[61,62] and monoclonal anti-NeuN (catalog no. MAB377; Chemicon International, Temecula, CA). After overnight incubation with primary antibodies at 4°C, sections were washed and processed using an avidin-biotin complex method. Signal was detected with 3,3′-diaminobenzidine tetrahydrochloride. Sections were counterstained with cresyl violet. Immunocytochemical controls consisted of either incubating tissue in nonimmune sera or omitting incubation in primary antisera (Supplemental Figure 1, see *http://ajp.amjpathol.org*).

### TUNEL

TUNEL was performed as described elsewhere.[63] Briefly, the sections were permeabilized with proteinase K (20 $\mu$g/ml), treated with RNAase A (100 $\mu$g/ml), and incubated with an equilibration buffer. The enzymatic reaction was performed for 1 hour at 37°C with the terminal deoxynucleotidyl transferase (TdT; catalog no. 3333566, Roche, Indianapolis, IN) and BODIPY TR-14-coupled dUTP (catalog no. C7618; Molecular Probe, Eugene, OR). The cyanine dye YOYO-1 (catalog no. Y3601, Molecular Probe) was used as a counterstain.

### *Ultrastructural Analyses*

For conventional electron microscopy (EM), PS/APP mice brains ($n = 4$, 16 months of age) were fixed by cardiac perfusion using 2% glutaraldehyde-4% paraformaldehyde in 0.1 mol/L sodium cacodylate buffer and postfixed in 1% osmium tetroxide. After alcohol dehydration, sections were embedded and ultrathin sections prepared and stained with uranyl acetate and lead citrate. Material was viewed with a Philips (Eindoven, Netherlands) CM 10 EM equipped with a Hamamatsu (Shizuoka, Japan) C4742-95 digital camera aided by AMT (Danvers, MA) Image Capture Engine software (version 5.42.443a). One-$\mu$m-thick sections were stained with toluidine blue for light microscopic examination.

A modified pre-embedding staining technique[64–66] was used for immunoelectron microscopy (IEM). PS/APP, WT mice of 24 months of age ($n = 4$ for each genotype), or neonatal C57BL/6J mice ($n = 3$) were perfused-fixed with 0.1% glutaraldehyde-4% paraformaldehyde in 0.1 mol/L sodium cacodylate buffer. The brains were removed and immersion-fixed for 4 hours at 4°C and subsequently transferred to 4% paraformaldehyde overnight at 4°C. Seventy-$\mu$m-thick vibratome sections were cut into phosphate-buffered saline (PBS), and treated with the following solutions alternating with PBS washes: 50% ethanol in PBS for 20 minutes, 0.05% Triton X-100 in PBS for 20 minutes, freshly made 1% sodium borohydride in PBS for 10 minutes, and 3% $H_2O_2$ for 10 minutes. After blocking the sections in 10% normal goat serum for 1 hour at room temperature, they were briefly rinsed and incubated in the anti-activated caspase-3 antibody [catalog no. 9661, Cell Signaling; diluted 1:200 in 1% bovine serum albumin (BSA)/PBS] overnight at 4°C. After washing in PBS, the sections were incubated in a biotinylated goat anti-rabbit secondary antibody (diluted 1:250 in 1% BSA/PBS; Vector Laboratories, Burlingame, CA) for 1 hour, then incubated in a Vector standard ABC solution (Vector Laboratories) for 2 hours, and reacted with 0.025% 3,3′-diaminobenzidine tetrahydrochloride in PBS in the presence of 0.006% $H_2O_2$ for 10 minutes. The 3,3′-diaminobenzidine tetrahydrochloride reaction product was then intensified with silver-gold treatment following the protocol from Teclemariam-Mesbah and colleagues.[65] The sections were then postfixed in 1% osmium tetroxide in 0.1 mol/L cacodylate buffer for 30 minutes, dehydrated in ethanol, and flat-embedded in resin. Areas of interest containing caspase-3-positive neuron(s) were first identified by light microscopy and ultrathin sections were placed on grids and not poststained. Note that optimization of immunolabeling by this technique requires fixation with very a low percentage of glutaraldehyde and treatment with Triton X-100, which results in suboptimal structural preservation.

Postembedding IEM with gold-conjugated secondary antibody was used to detect activated caspase-3 immunoreactivity in dystrophic neurites because this method allowed us to use conventional EM tissues (see above) fixed with high concentration of glutaraldehyde (ie, 2% in this study), which best preserves membrane structures. Ultrathin sections were placed on nickel grids, air-dried, and etched briefly with 1% sodium metaperiodate in PBS followed by washing in filtered double-distilled water and incubated with 1% BSA for 2 hours. Sections then were incubated overnight in the anti-activated caspase-3 antibody (1:50) in a humidified chamber overnight at 4°C, washed in PBS, and incubated in a secondary antibody conjugated with 15-nm gold particles (Amersham, Buckinghamshire, UK) for 2 hours at room temperature. Grids were washed and briefly stained with uranyl acetate and lead citrate before examination. Immunocytochemical controls consisted of either incubating tissue in nonimmune sera or omitting incubation in primary antisera (Supplemental Figure 1, see *http://ajp.amjpathol.org*).

### *Acid Phosphatase Histochemistry*

Enzyme histochemistry for acid phosphatase was performed using a lead capture technique with cytidine 5′-monophosphate as the substrate as previously described.[67] Sections were postfixed in 1% osmium tetroxide and processed for EM embedding.

### *Intracerebroventricular Infusion of Leupeptin*

Leupeptin (10 mg/ml in HEPES) or HEPES was infused into the lateral ventricle of 6-month-old PS/APP or WT mice ($n = 6$ for each treatment of each genotype) for a period of 2 weeks using an Alzet osmotic pump brain infusion kit (Alza, Mountain View, CA) with model 2004 miniosmotic pumps (0.25 $\mu$l/hour delivery rate). Alzet pumps were loaded with leupeptin or HEPES and connected to the brain infusion assembly with polyethylene tubing and incubated in sterile saline at 37°C for 48 hours before implant. Mice were anesthetized with pentobarbital (40 to 50 mg/kg i.p.) and placed in a stereotaxic apparatus with a mouse adapter (David Kopf Instruments, Tujunga, CA). The scalp was shaved and a midline incision made starting slightly behind the eyes, exposing the skull area. Through this opening, a hemostat was used to open a pocket on the back of the mouse to house the pump. The pump was inserted and its tubing length cut to fit the cannula, while still allowing free movement. The coordinates for the cannula placement in the lateral ventricle were AP −0.22 mm to bregma, ML 1.0 mm to bregma, and DV 2.5 mm to cranium. Cannula length was adjusted with spacers, or cannulas were made to order from Plastic Products Co. (Lindstrom, MN), thereby minimizing assembly protrusion. A hole was drilled in the skull, the cannula was glued to the cleaned and scraped skull with Loctite 454 (Henkel Technologies, Irvine, CA), and the incision closed over the assembly.

### *Immunoblotting*

Samples for cleaved caspase-3 Western blotting were prepared by homogenizing brains from leupeptin- or HEPES-infused mice in a tissue-homogenizing buffer (250 mmol/L sucrose, 20 mmol/L Tris, pH 7.4, 1 mmol/L EDTA, 1 mmol/L EGTA) containing protease inhibitors. The samples were diluted with 2× sample buffer and

heated for 10 minutes at 95°C, then vortexed for ~15 seconds to shear DNA. Forty μg of each sample were loaded into a 16% Tris-glycine gel (catalog no. EC6498BOX; Invitrogen, Carlsbad, CA), and then the gels were transferred to 0.2-μm nitrocellulose membranes. The blots were blocked for 1 hour in 5% nonfat milk in Tris-buffered saline (TBS), rinsed in TBST (TBS + 0.1% Tween-20), then incubated with a polyclonal antibody for cleaved caspase-3 (catalog no. AF835; R&D Systems, Minneapolis, MN) diluted 1:250 in TBS with 1% BSA and 0.1% Tween-20 overnight at 4°C. The membrane was washed three times in TBST then incubated in the donkey anti-rabbit horseradish peroxidase-conjugated secondary antibody (catalog no. 711-035-152; Jackson ImmunoResearch Laboratories, West Grove, PA), diluted 1:7500 in TBS with 1% BSA and 0.1% Tween-20, for 1 hour at room temperature. The membrane was again washed and then incubated in a Western Lightning chemiluminescence reagent (catalog no. NEL100; Perkin Elmer, Emeryville, CA) for 1 minute and exposed to film.

## Results

### Neuronal Apoptosis in Neonatal Mouse Brains

We used multiple approaches to study the mode(s) of neurodegeneration that exists in the brains of adult PS/APP mice. To demonstrate the validity of the various methods used here for detecting neuronal apoptosis, we first applied them to brains of neonatal (P5) WT mice, as positive controls, where programmed neuronal death by apoptosis is well established.[68–70] We identified numerous TUNEL-positive neurons in sections of the cerebral cortex (Figure 1A) and cerebellum (not shown) from the neonatal brains. On the same sections, the compact nuclei identified by TUNEL, also stained with the DNA-binding cyanine dye YOYO-1 (Figure 1B) and showed the condensed nuclear chromatin pattern associated with apoptosis in these cells. Additional histological evidence of nuclear condensation in the neonatal brain tissue was seen using Nissl stain (Figure 1A, inset). Immunocytochemical analysis using the neuronal marker, NeuN, confirmed the TUNEL-YOYO staining in these animals and revealed many atrophic neuronal profiles in neonatal mouse brains at P5 (not shown).

We next probed for the activation of caspases in degenerating neurons, a biochemical change associated with apoptotic cell death, using immunocytochemistry and antibodies recognizing the activated form of caspase-3 or a caspase-specific cleavage product of α-spectrin. Antibodies to activated caspase-3 immunolabeled a small number of scattered, distinct neurons in the cerebral cortex (Figure 1C) and other brain regions including cerebellum, hippocampus, striatum, and thalamus (not shown) and activated caspase-3 immunoreactivity was concentrated both in perikaryon and processes of degenerating neurons, similar to that seen in previous studies.[71] The morphology of caspase-3-positive neurons ranged from normal appearing neurons with elaborate neuritic arbors to small, shrunken cell bodies with apparently fragmented processes, clearly indicating ongoing degeneration. The morphologies of activated caspase-labeled cell bodies/nuclei included other typical apoptotic features such as marginalized chromatin, fragmented nuclei and apoptotic bodies (eg, Figure 1C, inset). Ab246, which detects caspase-cleaved α-spectrin fragments, revealed similar apoptotic features in degenerating neurons in the neonatal brain including small, condensed cell bodies, apoptotic bodies, and fragmented neuronal processes (Figure 1D).

To establish ultrastructural criteria for *in vivo* neuronal apoptosis to be applied to our later EM study in the PS/APP brains, we performed conventional EM analyses on neonatal mouse brains. These analyses revealed neurons with typical apoptotic features (Figure 2, A–D) strongly resembling those described for developmentally-regulated apoptosis in infant rat brains or induced apoptosis by head trauma or by drug treatments in rat and mouse brains.[34] The most striking apoptotic changes involved nuclei, including the formation of one or more CBs with different sizes and densities (Figure 2, A–C) and migration of chromatin to the periphery or one pole of the nucleus (Figure 2D). Nucleolar disassociation was also detectable (Figure 2B, arrow). Nuclear membrane was either visible (Figure 2A), fragmented, or undetectable (Figure 2, B and C) depending on the stage of the apoptotic degeneration. Detected cytoplasmic features were variable, ranging from intact organelles (Figure 2, A and C) to nondescript particulate or membranous debris with only a small number of visible organelles (Figure 2B), depending on the stage of apoptosis and was influenced by the plane of section of the cells as described previously.[34] CBs surrounded by a small amount of condensed cytoplasmic components (Figure 2C) may represent apoptotic bodies once they were pinched off from the cell.

We next performed pre-embedding immunogold cytochemistry on sections of neonatal brains with an antibody directed against activated caspase-3 to verify whether or not caspase-3-positive neurons undergo similar apoptotic changes to those detected by conventional EM, particularly alterations in nuclear morphology. As shown in Figure 2, E and F, activated caspase-3-positive neurons, whose perikarya were usually smaller or shrunken, contained silver-gold labeling particles throughout the cytoplasm and within the nucleus, but the neighboring normal neurons were unlabeled, underscoring the specificity of immunogold labeling for caspase-3-positive nuclei in apoptotic neurons. The caspase-3-positive neurons exhibited typical patterns of apoptotic nuclear change including margination of chromatin (Figure 2, E1 and E2) and formation of compacted CBs (Figure 2, E2, F1, and F2). The cell depicted in Figure 2F2 is the one in Figure 2F1 but on a separate ultrathin section and stained with uranyl acetate. The black appearance of the CBs in Figure 2F2 indicated that the gray appearance of CBs and marginated chromatin in Figure 2, E2 and F1, as a result of the omission of poststaining with either uranyl acetate or lead citrate, did represent condensed chromatin masses. The nuclear membrane was either visible (Figure 2E2) or undetectable (Figure 2, F1 and F2). The cytoplasm con-

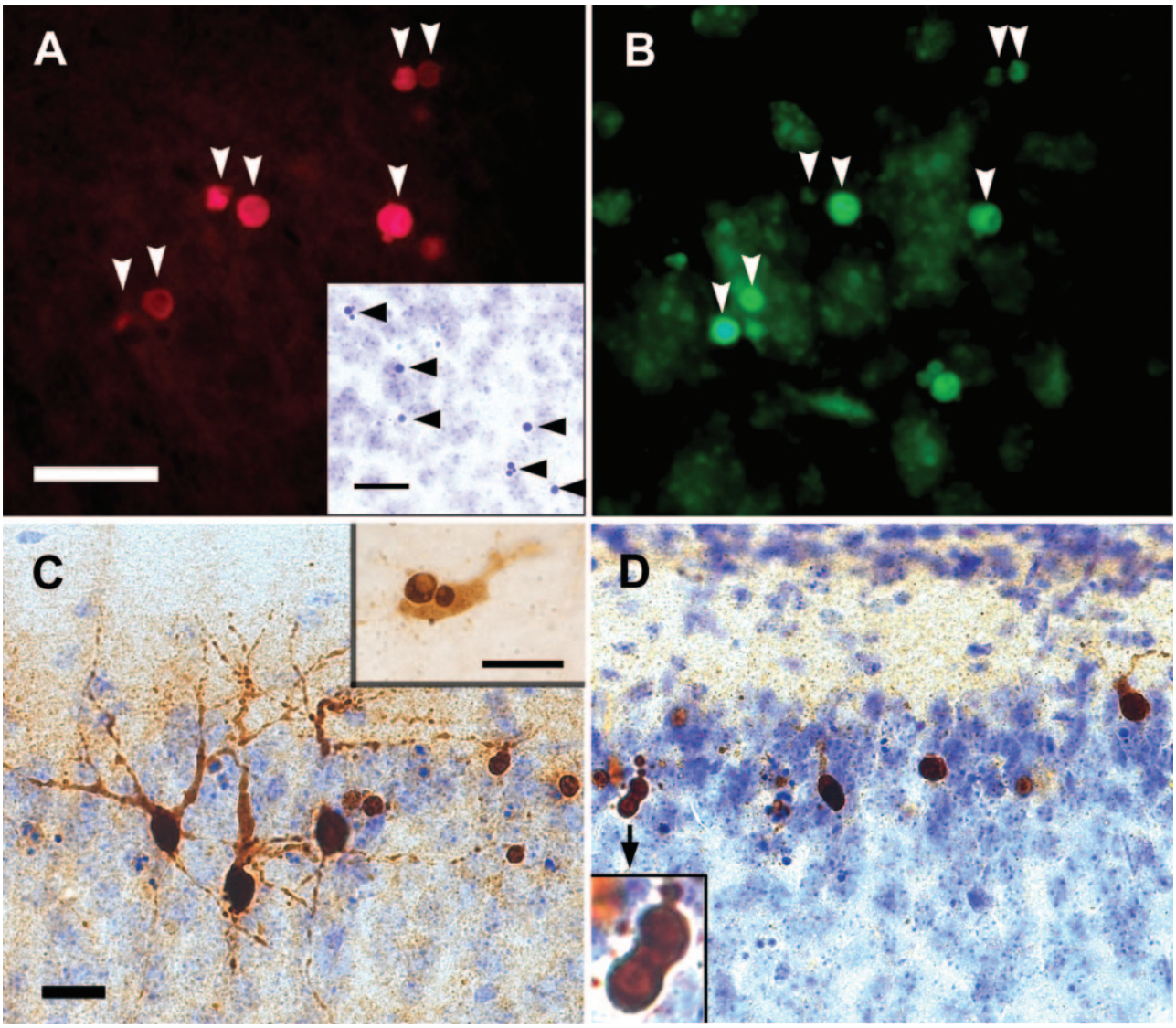


**Figure 1.** Apoptosis in the neonatal mouse brain. Sections of the cerebral cortex from neonatal brains stained by the TUNEL method (**A**) and by conventional microscopy with cresyl violet (**A**, **inset, black arrowheads**) reveals the presence of apoptotic nuclei (**white arrowheads**). The same sections counterstained with the DNA-binding dye YOYO-1 (**B**) show nuclear chromatin condensation (**white arrowheads**)—a structural change consistent with apoptosis. Increased caspase activity, a biochemical event associated with apoptosis, was detected using antibodies to activated caspase-3 (**C**) or Ab246, which detects caspase-cleaved $\alpha$-spectrin fragments (**D**), which intensely stained populations of apoptotic neurons and small intraneuronal spheroids that may represent the formation of apoptotic bodies (**C**, **inset**). **Inset** in **D** denotes that Ab246 immunostaining is predominantly within cytoplasm. However, because of the strong staining nature and the thickness of the sections (ie, 40 $\mu$m) it is difficult to determine whether the nucleus (in a dumbbell shape because of apoptotic nuclear changes) is also immunostained. Scale bars = 20 $\mu$m.

tained relatively intact cytoplasmic organelles (Figure 2E2), or particulate or membranous debris (Figure 2F1), unlike neurons that undergo necrotic cell death in which cytoplasmic organelles are usually lysed. The affected cells did not display large accumulations of AVs typical in autophagic cell death. These results, similar to those revealed by conventional EM (Figure 2, A–D), confirmed that activated caspase-3 immunostaining does signify ongoing apoptotic ultrastructural changes rather than merely reflecting caspase activation. Moreover, the results show that pre-embedding IEM with anti-caspase-3 antibody can be a useful tool for detecting neurons undergoing apoptosis that are technically very difficult to be detected by conventional EM analysis because of their rare occurrence in the PS/APP brain (see below).

### *Detection of Apoptotic Neurons in PS/APP Brains*

Using the same techniques, we examined the brains of WT and PS/APP mice at 6, 16, and 21 to 26 months of age. TUNEL revealed the presence of isolated positive, small, compact cell bodies/nuclei in the brains of the older PS/APP mice (Figure 3A1). The nuclei of these same cells were also stained with the DNA-binding cyanine dye YOYO-1 (Figure 3A2). Immunocytochemistry with anti-activated caspase-3 (Figure 3, B1 and B2) or Ab246 (Figure 3, C1 and C2)

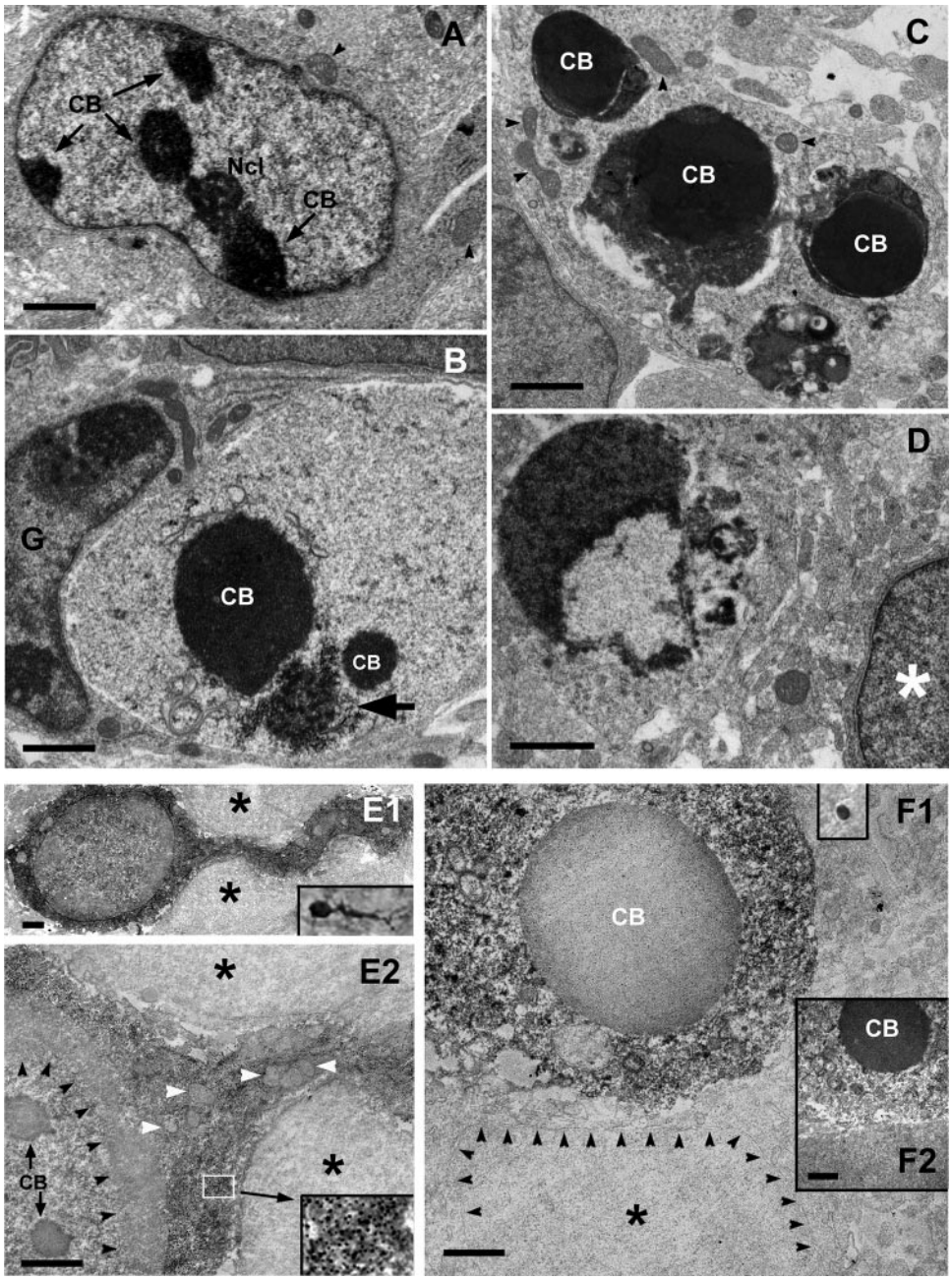


**Figure 2.** Apoptosis in the neonatal mouse brain: ultrastructural features. **A–D:** Electron micrographs from conventional EM analysis depicting typical neuronal apoptotic features. **A:** A neuron in an early apoptotic stage containing condensed small CBs in the nucleus. The nuclear membrane is intact and cytoplasmic organelles such as mitochondria (**arrowheads**) are relatively normal. Ncl, nucleolus. **B:** Depiction of later stage apoptotic changes in a neuron surrounded by a glial cell (G). Two CBs are highly packed and electron-dense, and the nucleolus (**arrow**) is undergoing separation of its elements. The nuclear membrane is not visible at this stage. The cytoplasm, intermixed with nucleoplasm, is undergoing transformation of its contents into nondescript particulate or membranous debris. **C:** Another late-stage apoptotic neuron containing three CBs, each surrounded by a small amount of condensed cytoplasmic components. **D:** On the **left** of the image, a neuron in the mid to late stage of apoptotic degeneration exhibits migration of chromatin to one pole of the nucleus; a normal neuronal nucleus (**asterisk**) is shown on the **right**. **E–F:** Electron micrographs from pre-embedding IEM depicting silver/gold-enhanced ultrastructural analyses of the same apoptotic neurons visualized by light microscopy after immunostaining with the anti-activated caspase-3 antibody (**insets** in **E1** and **F1**). To enable better signal (ie, 3,3′-diaminobenzidine tetrahydrochloride product/silver-gold particles representing the immunostaining) to background ratio, ultrathin sections were usually unstained with either uranyl acetate or lead citrate as in **E** and **F1**. The apoptotic neurons display strong caspase-3 immunoreactivity as indicated by silver-gold particles (**E2** and **F1**) (compare with the unlabeled neighboring normal neurons; **asterisks** in **E1**, **E2**, and **F1**). **E2** is a higher magnification photomicrograph of **E1**, depicting an immunolabeled neuron (**left**) in the early apoptotic stage exhibiting two small CBs and marginated chromatin in the nuclear periphery (**arrowheads**), visible nuclear membrane, and relatively unaltered cytoplasmic organelles (**white arrowheads**). **F2**, taken from a uranyl acetate-stained ultrathin section, shows the same apoptotic neuron as the one in **F1** (**top** in both images) to denote that the CB is highly electron-dense and condensed, similar to CBs revealed by conventional EM (**A–C**). Nuclear membrane of the apoptotic neuron in **F1** and **F2** has become fragmented and undetectable, in contrast to the intact nuclear membrane (**arrowheads** in **F1**) in the neighboring normal neuron (**asterisk**). Although some cytoplasmic organelles remain in the apoptotic neuron in **F1** (left side of the cell), the majority of the cytoplasm contained particulate or membranous debris. Note that empty space seen between apoptotic neurons and their neighboring cells is usually because of shrinkage of the apoptotic cells—one of the apoptotic features. Scale bars = 1 $\mu$m.

detected isolated immunoreactive neurons similar to those seen by TUNEL-YOYO scattered throughout the brains of PS/APP mice. The majority of caspase-3-immunoreactive neurons were grossly shrunken or fragmented without recognizable processes (Figure 3, B1 and B2), but some apparently intact cells were also observed (Figure 3, B1 and B2, insets). Similar to the patterns found in neonatal brains, in the brains of PS/APP mice, Ab246 immunoreactivity was predominantly found in condensed cell bodies (Figure 3C1, inset) or fragmented profiles that may represent apoptotic bodies (Figure 3, C1 and C2), without detectable immunolabeled processes. Double-label immunofluorescence with antibodies to activated caspase-3 and NeuN (Figure 3D) revealed that 89% of caspase-3-stained cells were also NeuN-positive, indicating the majority of caspase-3-positive cells detected were neurons. Morphometric analysis of the numbers of apoptotic neurons in the cortex and the hippocampus detected by TUNEL (not shown), activated caspase-3 antibody (Figure 3E), or Ab246 (not shown) in brain sections from PS/APP mice ranging in age from 6 to 26 months showed that apoptotic profiles were twofold higher in the 6- and 16-month groups and eightfold greater in the 21- to 26-month group compared to age-matched control mice (Figure 3E).

Neurons positive for a number of activated caspases have previously been detected in the AD brain, however, apoptosis has not been unequivocally established as a mechanism for neuronal cell death in AD attributable in part to the lack of evidence linking caspase activation with typical apoptotic ultrastructural morphology. We, therefore, performed additional analyses at the ultrastructural level to demonstrate both caspase activation and typical apoptotic morphology concurrently in brain sections from PS/APP mice.

Given that the number of caspase-3-positive apoptotic cells in each vibratome section is small as shown in Figure 3E, the estimated ratio of the total volume for all caspase-3-stained cells in the 21- to 26-month-old group to the total volume of cortex and hippocampus in each section is ~1 in 33,000, which makes detecting apoptotic neurons by conventional EM unfeasible. Therefore, we performed ultrastructural analyses of brain sections from 24-month-old PS/APP mice using a pre-embedding immunogold technique. We used the anti-caspase-3 antibody that was validated in neonatal brains (Figure 2) to

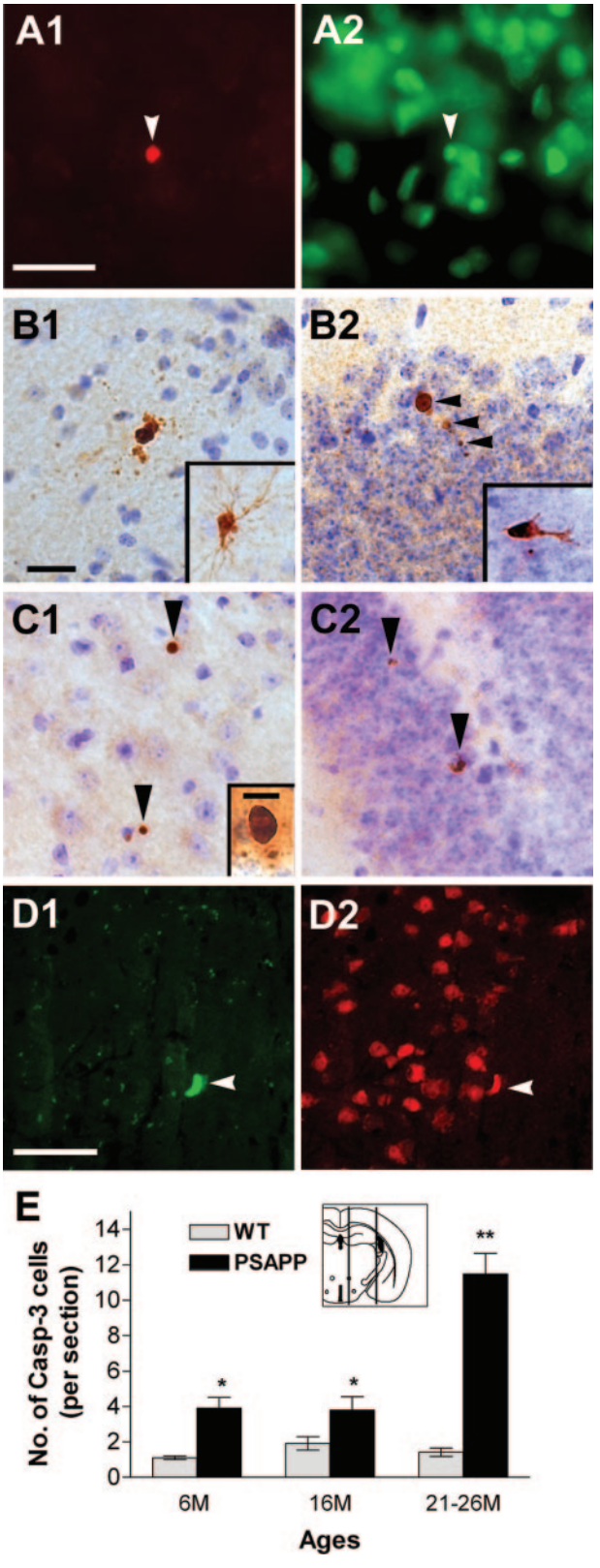


**Figure 3.** Detection of apoptotic neurons in the PS/APP brain. In brain sections from 16-month-old PS/APP mice, TUNEL-positive cells like the one represented in **A1** (**arrowhead**) are also visible by YOYO-1 (**A2**, **arrowhead**). Activated caspase-3 (**B**) and Ab246-positive cells (**C**, **arrowheads**) could be seen in the cortex (**B1**, **B1 inset**, **C1**, and **C1 inset**) and hippocampus (**B2**, **B2 inset**, and **C2**). The small round immunostained profiles in **B2**, **C1**, and **C2** may represent apoptotic bodies rather than whole cells. **Inset** in **C1** denotes that Ab246-immunostaining is predominantly within cytoplasm. However, because of the strong staining nature and the thickness of the sections (ie, 40 $\mu$m) it is difficult to determine whether or not the nucleus (the lighter area in the upper part of the cell) is also immunostained. Double-label immunofluorescence with anti-activated caspase-3 (**D1**) and anti-NeuN (**D2**) detects cells positive for both NeuN and caspase-3 (**arrowheads**). In **E**, morphometric analysis of activated caspase-3-positive apoptotic cells in the cortex and hippocampus of both WT and PS/APP ($n$ = 4 each genotype for the 6- and 16-month-old groups, five sections each mouse; $n$ = 8 each genotype for the 21- to 26-month-old group, two to five sections each mouse) was performed from sagittal brain sections obtained, with equal spacing, from the region between lateral 0.48 mm and lateral 2.16 mm of Paxinos and Franklin, 2001,[108] ie, the region between the two straight vertical lines shown in the **inset**. The average number of positive cells per section obtained for each animal was then used to calculate the mean ± SEM for each group. Data were analyzed by unpaired Student's $t$-test. $^{*}P < 0.05$, $^{**}P < 0.0001$. Scale bars: 20 $\mu$m (**A–C**, the bar in B1 is also for C1); 10 $\mu$m (**C1 inset**); 50 $\mu$m (**D**).

detect apoptotic morphologies at the ultrastructural level, which we found to be similar to those revealed by conventional EM. Thus, in addition to silver-gold immunolabeling throughout the cytoplasm and within the nucleus, caspase-3-positive neurons in the PS/APP brain exhibited ultrastructural features of apoptosis similar to those found in the neonatal brains: chromatin condensation, formation of highly compacted CBs (Figure 4, A and B; Supplemental Figure 2, see *http://ajp.amjpathol.org*), nuclear membrane fragmentation (Figure 4A2; Supplemental Figure 2, see *http://ajp.amjpathol.org*), and distortion of nuclei (Figure 4B). In addition, depending on the stage in the apoptotic degeneration, the cytoplasm in the apoptotic cells contained relatively intact cytoplasmic organelles (Figure 4A2) or particulate or membranous debris (Figure 4B).

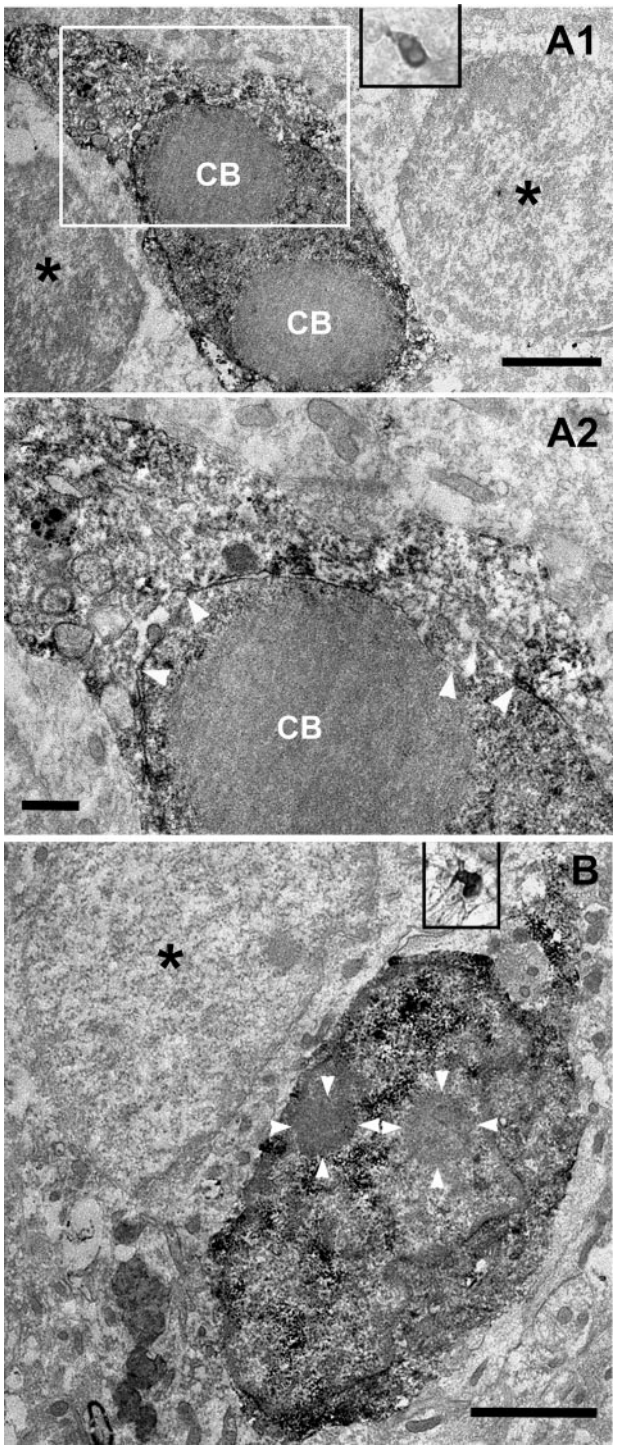


## *Additional Caspase-3-Independent Neuronal Degeneration in PS/APP Brains*

Occasional neurons in brain sections of older PS/APP mice stained with anti-NeuN antibody (not shown) or toluidine blue (Figure 5A) displayed abnormal morphological changes such as cell shrinkage, condensed nuclei and cytoplasmic organelles, and evidence of plasmalemmal blebbing. These features and the appearance of corkscrew-like dendrites in some neurons corresponded to the so-called "dark neurons" previously described.[72–74] At the EM level, dark neurons in PS/APP brains displayed electron-dense nucleus and cytoplasm (Figure 5, B–D), distorted nuclei (Figure 5B), dilated Golgi apparatus, mitochondria and endoplasmic reticulum (Figure 5, B and D2; white arrowheads), and accumulation of lysosomal compartments such as lipofuscin, which were reactive when stained for enzyme cytochemical evidence of lysosomal acid hydrolase activity (Figure 5C, white arrows). Although the nuclei appeared to be abnormal, ie, distorted and the whole nucleus evenly condensed, dark neurons usually did not display CBs. On sections processed with anti-activated caspase-3 antibody, few, if any, silver-gold particles were detected in dark neurons (Figure 5, D1 and D2) indicating that caspase-3 is not activated in the dark neurons.

## *Protein Markers of Apoptosis Are Present in Dystrophic Neurites in PS/APP Brains*

In addition to caspase-3-positive perikarya, immunocytochemical analyses using activated caspase-3 (Figure 6, D and E) or Ab246 (Figure 6F) antibodies in brain sections from 21- to 26-month-old PS/APP revealed intense

**Figure 4.** Ultrastructural analysis of activated caspase-3-positive neurons in the PS/APP brain. Brain sections of PS/APP and WT mice were processed for pre-embedding IEM using anti-activated caspase-3 antibody. **A** and **B:** Electron micrographs from PS/APP brains are shown. **Insets** in **A1** and **B** are light microscopic photomicrographs from resin-embedded sections showing caspase-3-positive neurons that were used to generate the ultrathin sections shown in **A1** and **B**. Ultrathin sections were not poststained with either uranyl acetate or lead citrate as explained in Figure 2. The apoptotic neurons display strong caspase-3 immunoreactivity as indicated by silver-gold labeling particles throughout the cytoplasm and within the nucleus (**A2** and **B**), but the neighboring normal neurons (**asterisks** in **A1** and **B**) are unlabeled. **A1:** A caspase-3-positive apoptotic neuron (center) contains two large-sized, highly compacted CBs (compare to the chromatin nature in the nuclei of neighboring neurons). **A2** is a higher magnification view of the boxed area in **A1** in which cytoplasmic organelles (as those in the top left of the cell) are still recognizable but discontinuous ends (**white arrowheads**) of the nuclear membrane are visible indicating ongoing nuclear membrane fragmentation. **B:** A caspase-3-positive apoptotic neuron (**right**) possesses a distorted nucleus containing two small CBs with different densities (each demarked by four **arrowheads**). Note that these nuclear features are completely different from what is seen in the neighboring normal neuron (**left**). The cytoplasmic organelles in the apoptotic neuron are undergoing transformation into particulate or membranous debris. Scale bars: 2 $\mu$m (**A1**, **B**); 500 nm (**A2**).

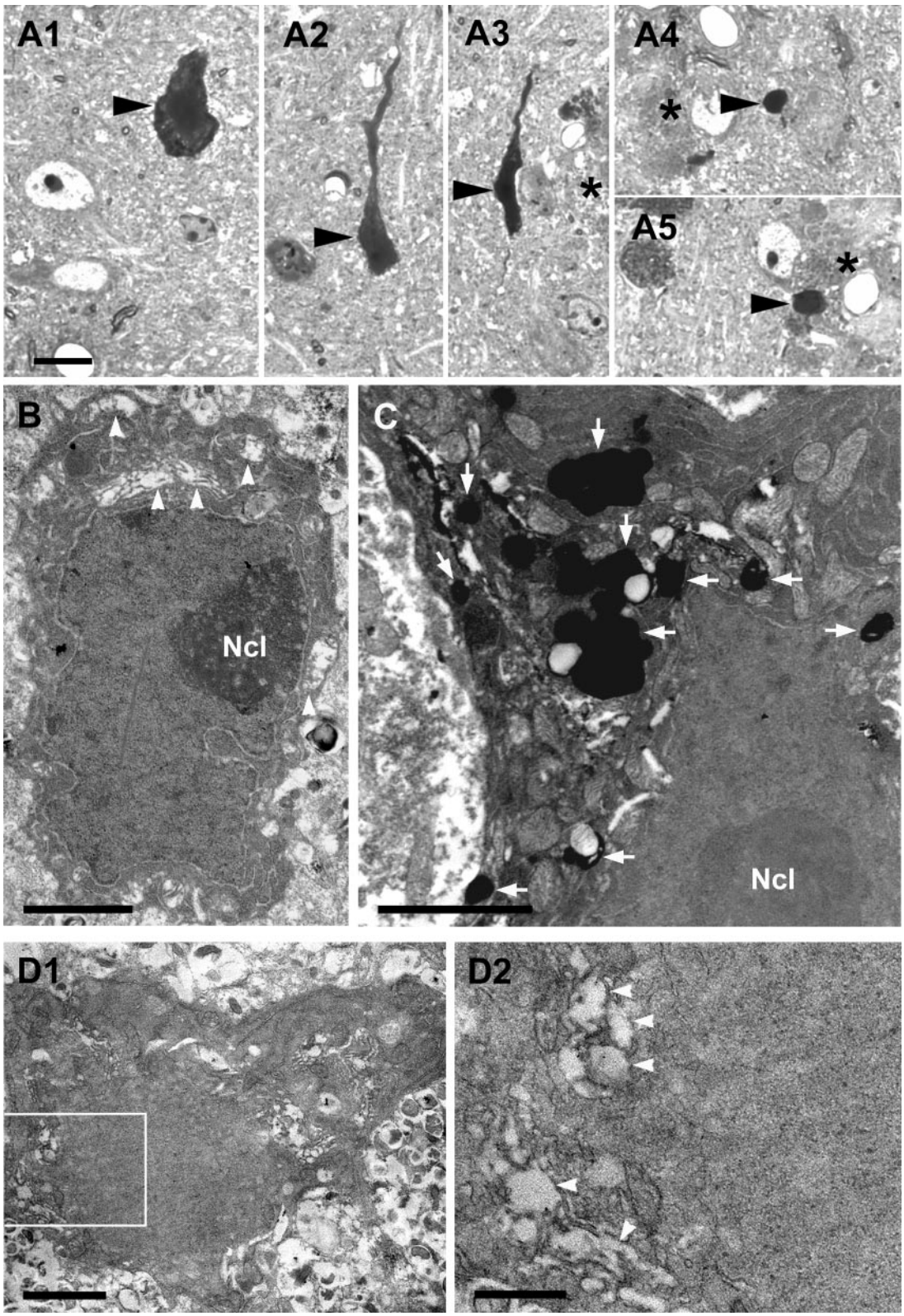


**Figure 5.** Dark degenerating neurons in the PS/APP brain. **A:** Toluidine blue-stained 1-$\mu$m-thick sections from 16-month-old PS/APP brains show intensely stained, shrunken neurons with various morphologies consistent with so-called dark neurons (**black arrowheads**). These degenerating cells were found throughout the cortical laminae and frequently were seen close to amyloid plaques (**A3–A5**, **asterisks**; the main portion of the plaque is not shown). Electron micrographs depict dark neurons from older PS/APP brains after conventional EM processing (**B**), pre-embedding histochemical staining for acid phosphatase (**C**), or pre-embedding IEM using anti-activated caspase-3 antibody (**D1**). The neuron depicted in **D1** was found on the same ultrathin section as the caspase-3-positive neuron shown in Figure 4A1. In the magnified boxed area of **D1** (**D2**), few, if any, silver-gold particles are evident within the cell (compare with magnified images in Figure 3). Scale bars: 10 $\mu$m (**A1–A5**); 2 $\mu$m (**B**, **C**, **D1**); 500 nm (**D2**). See text for description of white arrowheads in **B** and **D2**, and for description of white arrows in **C**.

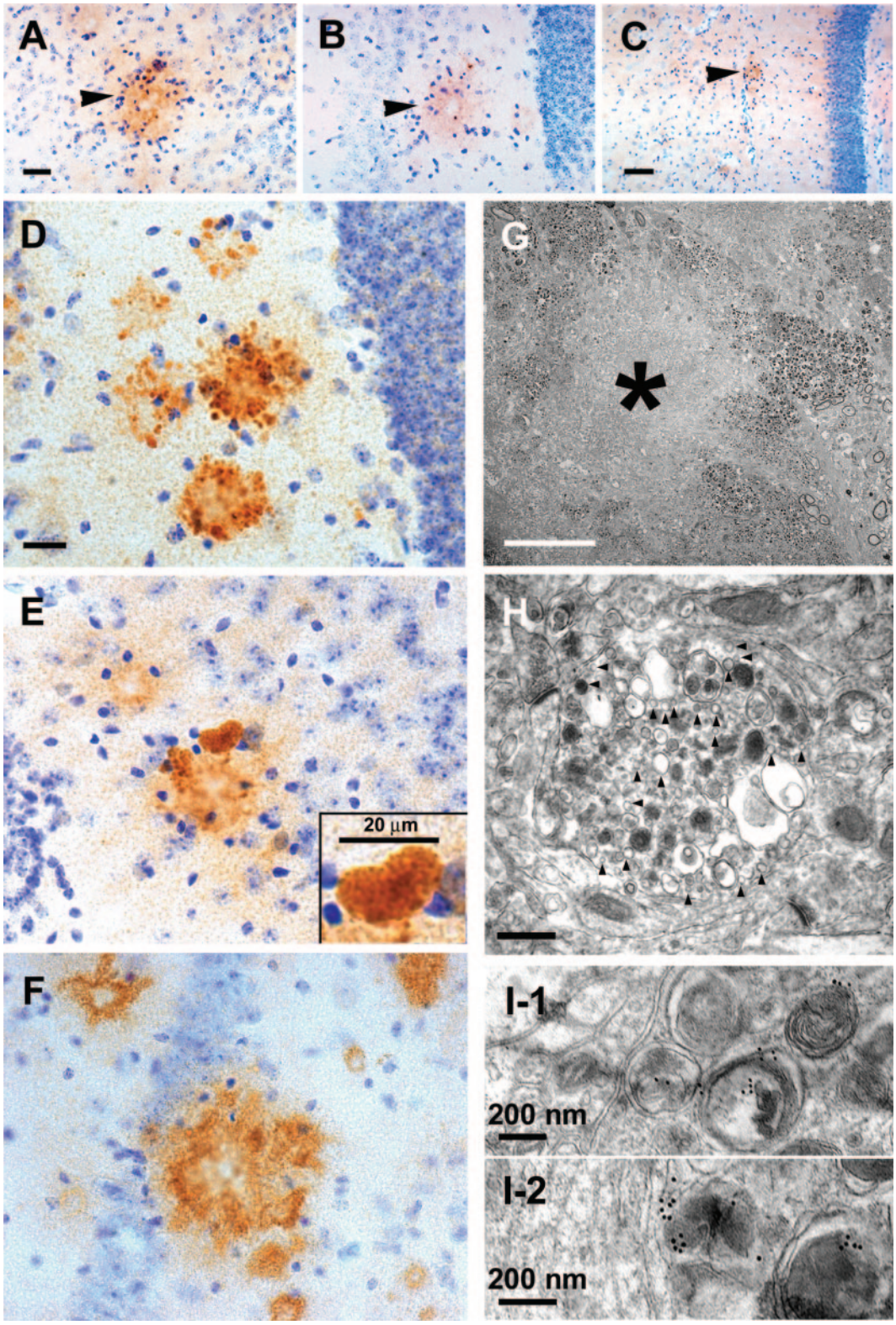


**Figure 6.** Protein markers of apoptosis are present in the dystrophic neurites in the PS/APP brain. Plaques (**arrowheads**) in the cortex (**A**) or hippocampus (**B** and **C**) of 6-month-old PS/APP brains show weak immunoreactivity for activated caspase-3 (**A** and **B**) or Ab246 (**C**). In brain sections from older 21- to 26-month PS/APP mice, amyloid plaques in the same brain regions are intensely immunoreactive with antibodies to activated caspase-3 antibody (**D** and **E**) or Ab246 (**F**), where labeling is stronger within degenerating neurites. Higher magnification photomicrographs of immunolabeled plaques (**inset** in **E**) reveals a punctate staining within a caspase-3-positive neuritic profile. Ultrastructural examination (**G** and **H**) shows that many dystrophic neurites are associated with the plaque corona (**asterisk** indicating the plaque core). At higher magnification (**H**), these neurites are filled predominantly with AVs (non-AV structures such as dense bodies, lysosomes, and synaptic vesicles are demarked with **arrowheads**). The AVs display caspase-3 immunoreactivity detected by postembedding immunogold labeling shown in **I1** and **I2**. Scale bars: 40 μm (**A**, **B**); 60 μm (**C**); 20 μm (**D–F**); 10 μm (**G**); 500 nm (**H**); 200 nm (**I**).

immunoreactivity for activated caspase-3 and caspase-cleaved spectrin in the neuritic compartments of numerous neuritic plaques of PS/APP mouse brains. In contrast, plaques in the brains of younger, 6-month-old PS/APP mice exhibited weak immunoreactivity to activated caspase-3 (Figure 6, A and B) or Ab246 (Figure 6C). Immunopositive regions in close proximity to the confines of the plaque and in the plaque corona were identified by ultrastructural examination as dystrophic neurites (Figure 6G). We found that the normal cytoplasmic content of these neurites was almost completely replaced by vesicular organelles (Figure 6H). In addition to small numbers of dense bodies, lysosomes, and synaptic vesicles, most of these organelles were AVs, based on their morphologies as previously described in this mouse model[56] and in the brains of AD patients.[55] Postembedding immunogold labeling with anti-activated caspase-3 antibody confirmed the localization of activated caspase-3 in dystrophic neurites and within the neurites, gold particles reflecting activated caspase-3 immunoreactivity (Figure 6, I1 and I2) were exclusively located in AVs.

### *Activated Caspase-3 Immunoreactivity Accumulates in AVs of Dystrophic Neurites when Autophagic Proteolysis Is Impeded*

The very striking localization of activated caspase-3 within AVs of dystrophic neurites, coupled with previous evidence that autophagic vacuole clearance is impaired in PS/APP mice and AD brain,[55,56] raised the possibility that autophagy is a pathway for eliminating apoptosis-inducing molecules such as caspases that might accumulate if autophagic digestion is impaired. To test this hypothesis, we infused leupeptin (10 mg/ml), an inhibitor of cysteine proteases, into the ventricles of WT or PS/APP brains for 2 weeks to impede proteolysis by the lysosomal cathepsin B, H, L, and S.[75,76] Leupeptin infusion in 6-month-old PS/APP brains induced increased caspase-3 immunolabeling in amyloid plaques, and strong immunostaining in hippocampal mossy fibers, ie, axons from the granule cells of the dentate gyrus, especially those located in the stratum lucidum of the hippocampal CA3 sector (Figure 7, B and C) compared to the PS/APP mice receiving HEPES vehicle (Figure 7A). Caspase-3 immunoreactivity also appeared in the same CA3 region of WT mice infused with leupeptin (not shown) but was consistently weaker than the staining observed in leupeptin-infused PS/APP. At the ultrastructural level, enlarged dystrophic neurites containing large numbers of AVs were detected in the stratum lucidum of the hippocampal CA3 sector in leupeptin-infused PS/APP (Figure 7D) or WT (not shown) mice. Within dystrophic neurites, activated caspase-3 immunoreactivity detected by immunogold EM was confined to AVs (Figure 7E). In addition to the hippocampal region, leupeptin infusion in 6-month-old PS/APP also induced caspase-3 immunoreactivity in many profiles in other brain regions including cortex, striatum, thalamus, and brainstem (Supplemental Figure 3, see *http://ajp.amjpathol.org*)—the number of caspase-3-positive neurons after leupeptin treatment was much larger compared to that in untreated PS/APP, which was usually less than five at this age as quantified in Figure 3E. Immunoblotting of brain homogenates (Figure 7F) using an anti-caspase antibody (catalog no. AF835, R&D Systems), which predominantly detects the 17-kDa fragment of activated caspase-3, revealed a higher level of the caspase-3 fragment in leupeptin-infused PS/APP brain sample than that from HEPES-infused PS/APP brain. Similarly, leupeptin-infusion into the WT brain increased the level of the caspase-3 fragment compared to that from HEPES-infused WT brain sample.

### *Leupeptin Treatment Accelerates Apoptosis*

The accumulation of activated caspase-3 in AVs within neuronal processes after leupeptin infusion (Figure 7; Supplemental Figure 3, see *http://ajp.amjpathol.org*) implied decreased caspase-3 clearance because of inhibition of autophagic-lysosomal function by leupeptin, which might cause increased apoptosis. This notion was supported by the observation of many caspase-3-positive profiles including neurons in various regions of leupeptin-infused brains (Supplemental Figure 3, see *http://ajp.amjpathol.org*). To further examine the extent of cell death induced by leupeptin, we performed TUNEL on leupeptin-infused brain sections compared with HEPES-infused sections (Figure 8). Many TUNEL-positive profiles were observed in leupeptin-treated PS/APP brain sections (>100 profiles per section). By contrast, only a very small number of TUNEL stained profiles (two to seven per section) was detected in HEPES-infused PS/APP brain sections. Almost all TUNEL-positive profiles were also stained by the DNA-binding dye YOYO-1 (Figure 8). The nature of condensation and fragmentation of TUNEL-positive nuclei, determined with the facilitation from the YOYO-1 counterstaining, suggested that the TUNEL-positive cells were undergoing apoptosis.

## *Discussion*

### *Apoptosis Is a Mode of Neuronal Cell Death in Aging PS/APP Mice*

In the relatively few investigations of neuronal cell death mechanisms in AD mouse models, apoptosis has been proposed as one mode of cell death in transgenic mice expressing an A$\beta$ minigene,[77] *PS1* mutations,[78] or *APP* with the Swedish double mutations.[79] The results of these studies were based primarily on TUNEL assay, which demonstrates DNA strand breaks, in affected neuronal populations. Because DNA damage occurs in apoptosis and necrotic types of cell death, however, TUNEL assay alone cannot definitively establish an apoptotic mechanism of cell death.[33,80,81] Rarely have multiple criteria been applied concurrently to brain tissues to establish modes of cell death unequivocally.

In our study, we used multiple approaches to show that neurodegeneration in the PS/APP mouse model of AD is associated with a series of typical morphological and

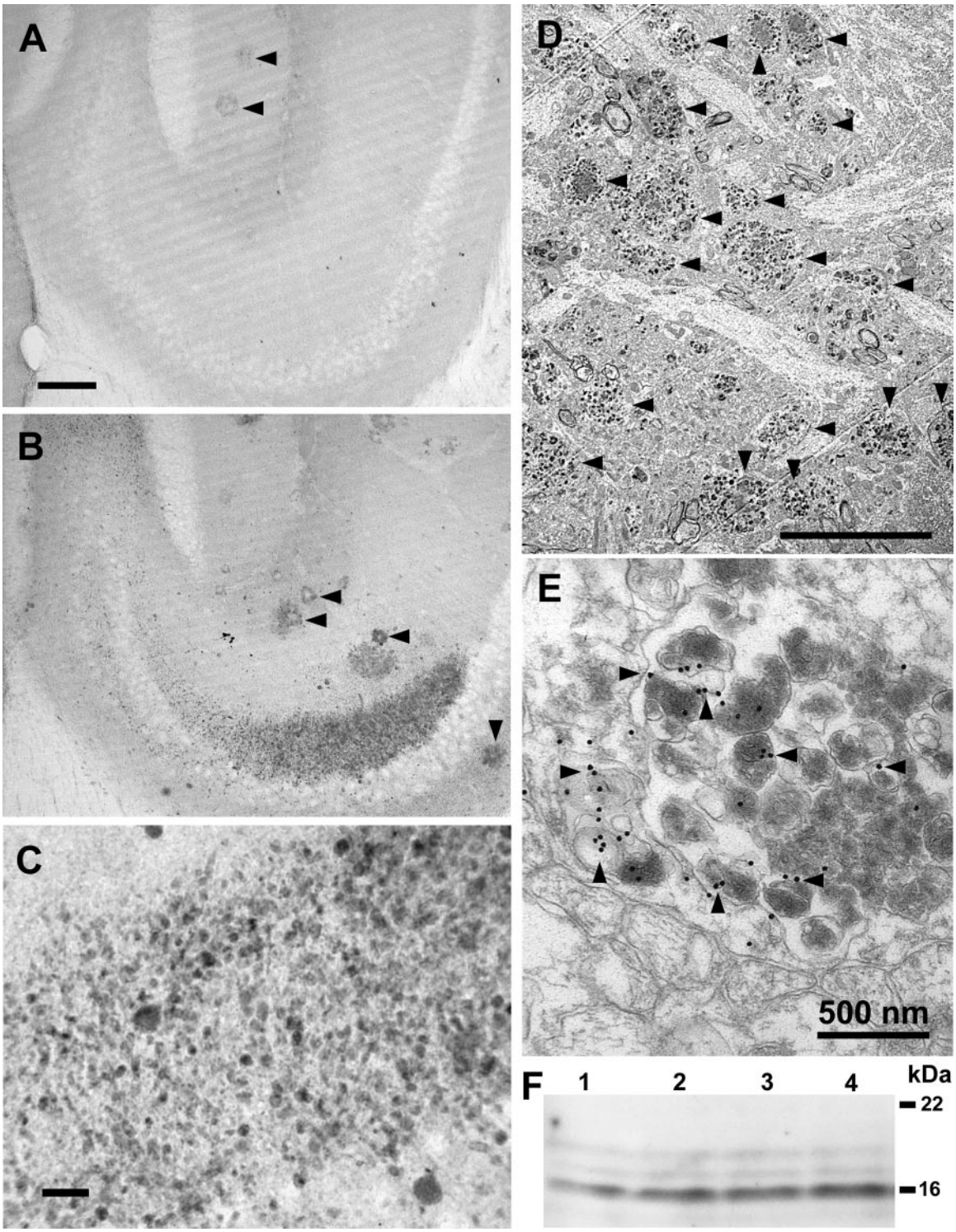


**Figure 7.** Activated caspase-3 immunoreactivity is prominent in AVs of dystrophic neurites after impeding lysosomal proteolysis *in vivo*. Immunocytochemical analysis reveals strong immunostaining for activated caspase-3 in neuronal processes in the hippocampus in leupeptin-infused 6-month-old PS/APP (**B**) mice. The stained neuronal processes span from the hilus of the dentate gyrus (**top left**; see Figure S3 for higher magnification view) to the stratum lucidum of the CA3 region (**bottom**), indicating that these processes are the hippocampal mossy fibers. Moderate or strong immunostaining is also observed in amyloid plaques (**arrowheads**). In contrast, HEPES-infused PS/APP mice (**A**) show no immunoreactivity in the same region except weak staining in amyloid plaques (**arrowheads**). Higher magnification photomicrographs of the stratum lucidum (**C**) demonstrates the distribution of caspase-3 immunolabeling to small, punctate profiles. EM analysis (**D**) of the section from the leupeptin-infused PS/APP mouse brain shown in **B** reveals dystrophic neurites (**arrowheads**) in the stratum lucidum. Postembedding immunogold labeling with the anti-activated caspase-3 antibody (**E**) shows the presence of caspase-3 (**arrows**) within the AVs in these dystrophic neurites. **F:** Immunoblotting of brain homogenates using an anti-caspase antibody predominantly detecting the 17-kDa fragment of activated caspase-3. **Lane 1:** HEPES-infused WT brain; **lane 2:** leupeptin-infused WT brain; **lane 3:** HEPES-infused PS/APP brain; **lane 4:** leupeptin-infused PS/APP brain. Scale bars: 60 $\mu$m (**A**, **B**); 20 $\mu$m (**C**); 10 $\mu$m (**D**); 500 nm (**E**).

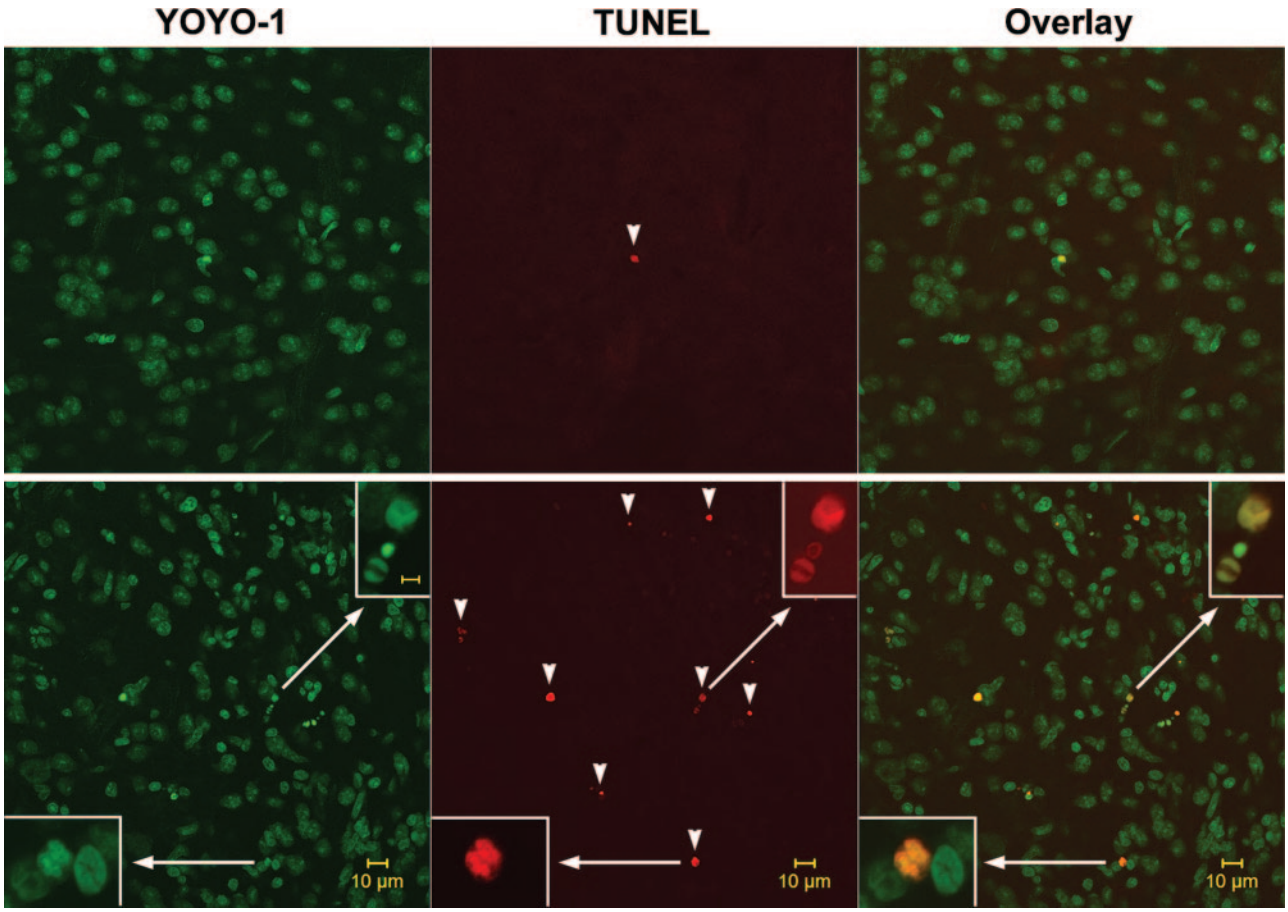


**Figure 8.** Leupeptin infusion induces apoptosis. Brain sections from HEPES-infused PS/APP (**top**) or leupeptin-infused PS/APP (**bottom**) were processed with TUNEL/YOYO-1 labeling. TUNEL-positive profiles (**arrowheads**), which are also stained with YOYO-1, are increased in leupeptin-infused brains compared to HEPES-infused brains. **Insets** in the **bottom** panels are higher magnification views showing condensation and fragmentation of TUNEL-positive nuclei. Scale bar = 2 $\mu$m (inside the **inset** at the **bottom left**).

biochemical features characteristic of apoptosis such as cell shrinkage, caspase activation, nuclear changes, and DNA fragmentation. Using TUNEL in combination with the cyanine nucleic acid dye, YOYO-1, to visualize chromatin condensation, and immunocytochemistry for activated caspase-3 and caspase-cleaved $\alpha$-spectrin, we identified at the light microscopic level small numbers of neurons undergoing apoptosis in affected regions of the PS/APP brain. These findings were verified using EM analysis. At the EM level, the same caspase-3-positive cells demonstrated nuclear chromatin condensation, clumping, and formation of CBs, together with nuclear membrane fragmentation. The use of pre-embedding IEM with anti-activated caspase-3 antibody therefore unequivocally linked proximal caspase activation to distal apoptotic nuclear morphology. These features of apoptosis closely resembled those that we observed in developmental neuronal cell death, a well-established model of apoptosis. To our knowledge, these results provide the first demonstration of IEM-verified apoptosis in this mouse model (ie, the PS/APP) of AD-related $\beta$-amyloidosis. Previous studies[58] of the PS/APP mice[57] described neurodegeneration and dark atrophic neurons, similar to our evidence for a second type of neurodegeneration also occurring in PS/APP mice (see below), but mode(s) of cell death had not been characterized by specific markers in the earlier study.

## *Multiple Distinct Modes of Neurodegeneration in the PS/APP Brain*

Although some neurons in PS/APP mice unequivocally undergo apoptosis, other neurons appear to degenerate by a different mechanism. In confirmation of previous studies of PS1 and PS/APP mice,[58,78] we observed neurodegeneration of the dark cell type, a poorly understood degenerative state. Dark degenerating neurons, or dark neurons, have been detected in various pathological conditions including ischemia, epilepsy,[73] and chronic neurodegenerative states, such as Huntington's disease and models of this disease.[74,82,83] Our data provide clear evidence that caspase-3 is minimally activated in neurons undergoing dark cell degeneration; however, it remains to be investigated whether or not dark cell degeneration leads to neuron loss and whether it represents a distinct type of neuronal cell death, a stage of apoptosis preceding the activation of caspase-3, or a form of apoptosis involving a different set of caspases.

The existence of at least two modes of neurodegeneration in the same mouse model underscores the complexity of cell death patterns in chronic neurodegenerative disease. Cross talk is extensive between different cell death pathways,[44,45,84–86] which include multiple types of caspase-dependent and caspase-independent programmed cell death,[87,88] as well as necrosis involving calpains and lysosomal cathepsins in AD brain and AD mouse models.[5,7,45,89] To determine the existence of other modes of neurodegeneration and to elucidate the cross talk between different cell death pathways in the brains of PS/APP mice will require further studies.

## *Autophagy—Apoptosis Cross Talk in the PS/APP Brain*

Autophagy plays roles in both cell survival and cell death, and its involvement in aging or neurodegenerative diseases such as Alzheimer's, Parkinson's, and Huntington's Diseases has recently gained attention.[45] In the brains of AD patients and AD-related APP or PS/APP mouse models, it is evident that AVs accumulate within enormously swollen dystrophic neurites,[55,56,90,91] which may reflect autophagy induction, but more significantly, imply impairment of the autophagy machinery in these pathological conditions.[90] A striking finding in our study was the accumulation of activated caspase-3 in AVs within dystrophic neurites associated with amyloid plaques of old PS/APP mice. These observations and the localization of immunoreactivity to caspase-cleaved $\alpha$-spectrin with activated caspase-3 in the plaques supports the idea that caspase-3 activation is unlikely to be occurring simply during the autophagic turnover of caspase but occurs, instead, before its autophagic sequestration. The moderate accumulation of caspase-3 in AVs of hippocampal neuronal processes in WT mice treated with leupeptin suggests that a low level of activated caspase-3 turnover by autophagy may be a normal process, although it is possible also that toxic effects of leupeptin induce this caspase-3 activation. The greater accumulation of activated caspase-3 in PS/APP mice and larger effect of leupeptin in promoting this phenomenon in various brain regions particularly in hippocampal neurons is consistent with a greater production and/or lesser turnover in PS/APP mice than in WT mice. The later possibility is strengthened by the observation that leupeptin increases the content of activated caspase-3 in AVs of dystrophic neuritis in amyloid plaques (Figure 7B) in PS/APP mice, which accords with other evidence that neuronal autophagy is impaired in dystrophic neurites, where maturation of autophagosomes to lysosomes is delayed and protein digestion is slowed.[92] Thus, in this situation, the effect of additional protease inhibition in these AVs deteriorates protein turnover.

Previous studies in AD brains have found that 13 to 20% of neurons in the CA1 and subiculum contain granules of granulovacuolar degeneration.[16] These are 1- to 5-$\mu$m cytoplasmic vesicles primarily found in the hippocampus, which may represent a specific type of AVs/autophagosomes.[93] Interestingly, granules in more than 50% of the granulovacuolar degeneration-containing neurons show immunoreactivity to activated caspase-3,[16,19,94] implying an interrelationship between apoptosis and autophagy. Therefore, the observation in our study that activated capase-3 accumulates in AVs in dystrophic neurites in PS/APP mouse brains, which is enhanced by leupeptin treatment, suggests that localization of activated caspase-3 in granulovacuolar degeneration may indicate impaired autophagic function such as slowed turnover of activated caspases in neurons of the hippocampal region in AD brains.

These findings, along with the observation that leupeptin induces TUNEL labeling in many condensed and/or fragmented nuclei (Figure 8), support growing evidence of cross talk between autophagy and apoptotic pathways[45,95–97] including the regulation of both apoptosis and autophagy by common regulatory factors such as growth factors, Bcl-2 protein, and ER stress[98–100]; anti-apoptotic effects of autophagy[51,101]; proapoptotic effects of defective autophagy[102,103]; and autophagy activation during the execution of apoptosis.[104–107]

In conclusion, the turnover of pro-apoptotic factors like activated caspase-3 by autophagy, as seen here, are consistent with a possible protective effect of autophagy against apoptosis. Our studies demonstrate the importance of using a validated battery of criteria to establish apoptosis in brain and to distinguish it from other patterns of cell death that may be occurring in some cell types as part of the same disease process. In addition, the studies underscore the concept that multiple proteolytic pathways may concurrently influence neuronal survival and the pattern of cell death in certain populations of neurons.

## *Acknowledgment*

We thank Nicole Piorkowski for assistance in manuscript preparation.

## *References*

1. Price JL, Ko AI, Wade MJ, Tsou SK, McKeel DW, Morris JC: Neuron number in the entorhinal cortex and CA1 in preclinical Alzheimer disease. Arch Neurol 2001, 58:1395–1402
2. Giannakopoulos P, Herrmann FR, Bussiere T, Bouras C, Kovari E, Perl DP, Morrison JH, Gold G, Hof PR: Tangle and neuron numbers, but not amyloid load, predict cognitive status in Alzheimer's disease. Neurology 2003, 60:1495–1500
3. Gómez-Isla T, Price JL, McKeel DW Jr, Morris JC, Growdon JH, Hyman BT: Profound loss of layer II entorhinal cortex neurons occurs in very mild Alzheimer's disease. J Neurosci 1996, 16:4491–4500
4. West MJ, Coleman PD, Flood DG, Troncoso JC: Differences in the pattern of hippocampal neuronal loss in normal ageing and Alzheimer's disease. Lancet 1994, 344:769–772
5. Saito K, Elce JS, Hamos JE, Nixon RA: Widespread activation of calcium-activated neutral proteinase (calpain) in the brain in Alzheimer disease: a potential molecular basis for neuronal degeneration. Proc Natl Acad Sci USA 1993, 90:2628–2632
6. Grynspan F, Griffin WR, Cataldo A, Katayama S, Nixon RA: Active site-directed antibodies identify calpain II as an early-appearing and pervasive component of neurofibrillary pathology in Alzheimer's disease. Brain Res 1997, 763:145–158
7. Nixon RA, Cataldo AM: Lysosomal system pathways: genes to neurodegeneration in Alzheimer's disease. J Alzheimers Dis 2006, 9:277–289
8. Rohn TT, Rissman RA, Head E, Cotman CW: Caspase activation in

the Alzheimer's disease brain: tortuous and torturous. Drug News Perspect 2002, 15:549–557
9. Cribbs DH, Poon WW, Rissman RA, Blurton-Jones M: Caspase-mediated degeneration in Alzheimer's disease. Am J Pathol 2004, 165:353–355
10. Cotman CW, Su JH: Mechanisms of neuronal death in Alzheimer's disease. Brain Pathol 1996, 6:493–506
11. Su JH, Anderson AJ, Cummings BJ, Cotman CW: Immunohistochemical evidence for apoptosis in Alzheimer's disease. Neuroreport 1994, 5:2529–2533
12. Lassmann H, Bancher C, Breitschopf H, Wegiel J, Bobinski M, Jellinger K, Wisniewski HM: Cell death in Alzheimer's disease evaluated by DNA fragmentation in situ. Acta Neuropathol (Berl) 1995, 89:35–41
13. Anderson AJ, Su JH, Cotman CW: DNA damage and apoptosis in Alzheimer's disease: colocalization with c-Jun immunoreactivity, relationship to brain area, and effect of postmortem delay. J Neurosci 1996, 16:1710–1719
14. Li WP, Chan WY, Lai HW, Yew DT: Terminal dUTP nick end labeling (TUNEL) positive cells in the different regions of the brain in normal aging and Alzheimer patients. J Mol Neurosci 1997, 8:75–82
15. Lucassen PJ, Chung WC, Kamphorst W, Swaab DF: DNA damage distribution in the human brain as shown by in situ end labeling; area-specific differences in aging and Alzheimer disease in the absence of apoptotic morphology. J Neuropathol Exp Neurol 1997, 56:887–900
16. Stadelmann C, Deckwerth TL, Srinivasan A, Bancher C, Bruck W, Jellinger K, Lassmann H: Activation of caspase-3 in single neurons and autophagic granules of granulovacuolar degeneration in Alzheimer's disease. Evidence for apoptotic cell death. Am J Pathol 1999, 155:1459–1466
17. Rohn TT, Head E, Nesse WH, Cotman CW, Cribbs DH: Activation of caspase-8 in the Alzheimer's disease brain. Neurobiol Dis 2001, 8:1006–1016
18. Rohn TT, Rissman RA, Davis MC, Kim YE, Cotman CW, Head E: Caspase-9 activation and caspase cleavage of tau in the Alzheimer's disease brain. Neurobiol Dis 2002, 11:341–354
19. Su JH, Kesslak JP, Head E, Cotman CW: Caspase-cleaved amyloid precursor protein and activated caspase-3 are co-localized in the granules of granulovacuolar degeneration in Alzheimer's disease and Down's syndrome brain. Acta Neuropathol (Berl) 2002, 104:1–6
20. Guo H, Albrecht S, Bourdeau M, Petzke T, Bergeron C, LeBlanc AC: Active caspase-6 and caspase-6-cleaved tau in neuropil threads, neuritic plaques, and neurofibrillary tangles of Alzheimer's disease. Am J Pathol 2004, 165:523–531
21. Gamblin TC, Chen F, Zambrano A, Abraha A, Lagalwar S, Guillozet AL, Lu M, Fu Y, Garcia-Sierra F, LaPointe N, Miller R, Berry RW, Binder LI, Cryns VL: Caspase cleavage of tau: linking amyloid and neurofibrillary tangles in Alzheimer's disease. Proc Natl Acad Sci USA 2003, 100:10032–10037
22. Cotman CW, Poon WW, Rissman RA, Blurton-Jones M: The role of caspase cleavage of tau in Alzheimer disease neuropathology. J Neuropathol Exp Neurol 2005, 64:104–112
23. Rohn TT, Head E, Su JH, Anderson AJ, Bahr BA, Cotman CW, Cribbs DH: Correlation between caspase activation and neurofibrillary tangle formation in Alzheimer's disease. Am J Pathol 2001, 158:189–198
24. Yang F, Sun X, Beech W, Teter B, Wu S, Sigel J, Vinters HV, Frautschy SA, Cole GM: Antibody to caspase-cleaved actin detects apoptosis in differentiated neuroblastoma and plaque-associated neurons and microglia in Alzheimer's disease. Am J Pathol 1998, 152:379–389
25. Gervais FG, Xu D, Robertson GS, Vaillancourt JP, Zhu Y, Huang J, LeBlanc A, Smith D, Rigby M, Shearman MS, Clarke EE, Zheng H, Van Der Ploeg LH, Ruffolo SC, Thornberry NA, Xanthoudakis S, Zamboni RJ, Roy S, Nicholson DW: Involvement of caspases in proteolytic cleavage of Alzheimer's amyloid-beta precursor protein and amyloidogenic A beta peptide formation. Cell 1999, 97:395–406
26. Ayala-Grosso C, Ng G, Roy S, Robertson GS: Caspase-cleaved amyloid precursor protein in Alzheimer's disease. Brain Pathol 2002, 12:430–441
27. Kerr JF, Wyllie AH, Currie AR: Apoptosis: a basic biological phenomenon with wide-ranging implications in tissue kinetics. Br J Cancer 1972, 26:239–257
28. Kroemer G, Dallaporta B, Resche-Rigon M: The mitochondrial death/life regulator in apoptosis and necrosis. Annu Rev Physiol 1998, 60:619–642
29. Saraste A, Pulkki K: Morphologic and biochemical hallmarks of apoptosis. Cardiovasc Res 2000, 45:528–537
30. Leist M, Jaattela M: Four deaths and a funeral: from caspases to alternative mechanisms. Nat Rev Mol Cell Biol 2001, 2:589–598
31. Ziegler U, Groscurth P: Morphological features of cell death. News Physiol Sci 2004, 19:124–128
32. Jellinger KA: Challenges in neuronal apoptosis. Curr Alzheimer Res 2006, 3:377–391
33. Roth KA: Caspases, apoptosis, and Alzheimer disease: causation, correlation, and confusion. J Neuropathol Exp Neurol 2001, 60:829–838
34. Dikranian K, Ishimaru MJ, Tenkova T, Labruyere J, Qin YQ, Ikonomidou C, Olney JW: Apoptosis in the in vivo mammalian forebrain. Neurobiol Dis 2001, 8:359–379
35. Budihardjo I, Oliver H, Lutter M, Luo X, Wang X: Biochemical pathways of caspase activation during apoptosis. Annu Rev Cell Dev Biol 1999, 15:269–290
36. Hengartner MO: The biochemistry of apoptosis. Nature 2000, 407:770–776
37. Guimarães CA, Linden R: Programmed cell death: apoptosis and alternative deathstyles. Eur J Biochem 2004, 271:1638–1650
38. Stefanis L: Caspase-dependent and -independent neuronal death: two distinct pathways to neuronal injury. Neuroscientist 2005, 11:50–62
39. Chang HY, Yang X: Proteases for cell suicide: functions and regulation of caspases. Microbiol Mol Biol Rev 2000, 64:821–846
40. Zhang J, Xu M: Apoptotic DNA fragmentation and tissue homeostasis. Trends Cell Biol 2002, 12:84–89
41. Wyllie AH: Glucocorticoid-induced thymocyte apoptosis is associated with endogenous endonuclease activation. Nature 1980, 284:555–556
42. Gavrieli Y, Sherman Y, Ben-Sasson SA: Identification of programmed cell death in situ via specific labeling of nuclear DNA fragmentation. J Cell Biol 1992, 119:493–501
43. Baehrecke EH: Autophagy: dual roles in life and death? Nat Rev Mol Cell Biol 2005, 6:505–510
44. Levine B, Yuan J: Autophagy in cell death: an innocent convict? J Clin Invest 2005, 115:2679–2688
45. Nixon RA: Autophagy in neurodegenerative disease: friend, foe or turncoat? Trends Neurosci 2006, 29:528–535
46. Blommaart EF, Luiken JJ, Meijer AJ: Autophagic proteolysis: control and specificity. Histochem J 1997, 29:365–385
47. Klionsky DJ, Ohsumi Y: Vacuolar import of proteins and organelles from the cytoplasm. Annu Rev Cell Dev Biol 1999, 15:1–32
48. Klionsky DJ, Emr SD: Autophagy as a regulated pathway of cellular degradation. Science 2000, 290:1717–1721
49. Larsen KE, Sulzer D: Autophagy in neurons: a review. Histol Histopathol 2002, 17:897–908
50. Cuervo AM: Autophagy: in sickness and in health. Trends Cell Biol 2004, 14:70–77
51. Lum JJ, Bauer DE, Kong M, Harris MH, Li C, Lindsten T, Thompson CB: Growth factor regulation of autophagy and cell survival in the absence of apoptosis. Cell 2005, 120:237–248
52. Clarke PG: Developmental cell death: morphological diversity and multiple mechanisms. Anat Embryol 1990, 181:195–213
53. Edinger AL, Thompson CB: Death by design: apoptosis, necrosis and autophagy. Curr Opin Cell Biol 2004, 16:663–669
54. Matyja E, Taraszewska A, Naganska E, Rafalowska J: Autophagic degeneration of motor neurons in a model of slow glutamate excitotoxicity in vitro. Ultrastruct Pathol 2005, 29:331–339
55. Nixon RA, Wegiel J, Kumar A, Yu WH, Peterhoff C, Cataldo A, Cuervo AM: Extensive involvement of autophagy in Alzheimer disease: an immuno-electron microscopy study. J Neuropathol Exp Neurol 2005, 64:113–122
56. Yu WH, Cuervo AM, Kumar A, Peterhoff CM, Schmidt SD, Lee JH, Mohan PS, Mercken M, Farmery MR, Tjernberg LO, Jiang Y, Duff K, Uchiyama Y, Naslund J, Mathews PM, Cataldo AM, Nixon RA: Macroautophagy—a novel beta-amyloid peptide-generating pathway activated in Alzheimer's disease. J Cell Biol 2005, 171:87–98
57. Holcomb L, Gordon MN, McGowan E, Yu X, Benkovic S, Jantzen P, Wright K, Saad I, Mueller R, Morgan D, Sanders S, Zehr C, O'Campo K, Hardy J, Prada CM, Eckman C, Younkin S, Hsiao K, Duff K:

Accelerated Alzheimer-type phenotype in transgenic mice carrying both mutant amyloid precursor protein and presenilin 1 transgenes. Nat Med 1998, 4:97–100
58. Kurt MA, Davies DC, Kidd M, Duff K, Rolph SC, Jennings KH, Howlett DR: Neurodegenerative changes associated with beta-amyloid deposition in the brains of mice carrying mutant amyloid precursor protein and mutant presenilin-1 transgenes. Exp Neurol 2001, 171:59–71
59. Sadowski M, Pankiewicz J, Scholtzova H, Ji Y, Quartermain D, Jensen CH, Duff K, Nixon RA, Gruen RJ, Wisniewski T: Amyloid-beta deposition is associated with decreased hippocampal glucose metabolism and spatial memory impairment in APP/PS1 mice. J Neuropathol Exp Neurol 2004, 63:418–428
60. Takeuchi A, Irizarry MC, Duff K, Saido TC, Hsiao Ashe K, Hasegawa M, Mann DM, Hyman BT, Iwatsubo T: Age-related amyloid beta deposition in transgenic mice overexpressing both Alzheimer mutant presenilin 1 and amyloid beta precursor protein Swedish mutant is not associated with global neuronal loss. Am J Pathol 2000, 157:331–339
61. Oo TF, Siman R, Burke RE: Distinct nuclear and cytoplasmic localization of caspase cleavage products in two models of induced apoptotic death in dopamine neurons of the substantia nigra. Exp Neurol 2002, 175:1–9
62. Zhang C, Siman R, Xu YA, Mills AM, Frederick JR, Neumar RW: Comparison of calpain and caspase activities in the adult rat brain after transient forebrain ischemia. Neurobiol Dis 2002, 10:289–305
63. Tatton NA, lean-Fraser A, Tatton WG, Perl DP, Olanow CW: A fluorescent double-labeling method to detect and confirm apoptotic nuclei in Parkinson's disease. Ann Neurol 1998, 44:S142–S148
64. Totterdell S, Ingham CA, Bolam JP: Immunocytochemistry I: preembedding staining. Experimental Neuroanatomy: A Practical Approach. Edited by Bolam JP. Oxford, Oxford University Press, 1992, pp 103–128
65. Teclemariam-Mesbah R, Wortel J, Romijn HJ, Buijs RM: A simple silver-gold intensification procedure for double DAB labeling studies in electron microscopy. J Histochem Cytochem 1997, 45:619–621
66. Talbot K, Cho DS, Ong WY, Benson MA, Han LY, Kazi HA, Kamins J, Hahn CG, Blake DJ, Arnold SE: Dysbindin-1 is a synaptic and microtubular protein that binds brain snapin. Hum Mol Genet 2006, 15:3041–3054
67. Cataldo AM, Paskevich PA, Kominami E, Nixon RA: Lysosomal hydrolases of different classes are abnormally distributed in brains of patients with Alzheimer disease. Proc Natl Acad Sci USA 1991, 88:10998–11002
68. Ferrer I, Soriano E, Del Rio JA, Alcantara S, Auladell C: Cell death and removal in the cerebral cortex during development. Prog Neurobiol 1992, 39:1–43
69. Oppenheim RW: Cell death during development of the nervous system. Annu Rev Neurosci 1991, 14:453–501
70. Nijhawan D, Honarpour N, Wang X: Apoptosis in neural development and disease. Annu Rev Neurosci 2000, 23:73–87
71. Olney JW, Tenkova T, Dikranian K, Muglia LJ, Jermakowicz WJ, D'Sa C, Roth KA: Ethanol-induced caspase-3 activation in the in vivo developing mouse brain. Neurobiol Dis 2002, 9:205–219
72. Auer R, Sutherland GR: Hypoxia and related conditions. Greenfield's Neuropathology. Edited by Graham DI, Lantos PL. New York, Arnold, 2002, pp 233–280
73. Graeber MB, Blakemore WF, Kreutzberg GW: Cellular pathology of the central nervous system. Greenfield's Neuropathology. Edited by Graham DI, Lantos PL. New York, Arnold, 2002, pp 123–191
74. Turmaine M, Raza A, Mahal A, Mangiarini L, Bates GP, Davies SW: Nonapoptotic neurodegeneration in a transgenic mouse model of Huntington's disease. Proc Natl Acad Sci USA 2000, 97:8093–8097
75. Katunuma N, Kominami E: Lysosomal sequestration of cytosolic enzymes and lysosomal thiol cathepsins. Adv Enzyme Regul 1985, 23:159–168
76. Hariri M, Millane G, Guimond MP, Guay G, Dennis JW, Nabi IR: Biogenesis of multilamellar bodies via autophagy. Mol Biol Cell 2000, 11:255–268
77. LaFerla FM, Tinkle BT, Bieberich CJ, Haudenschild CC, Jay G: The Alzheimer's A beta peptide induces neurodegeneration and apoptotic cell death in transgenic mice. Nat Genet 1995, 9:21–30
78. Chui DH, Tanahashi H, Ozawa K, Ikeda S, Checler F, Ueda O, Suzuki H, Araki W, Inoue H, Shirotani K, Takahashi K, Gallyas F, Tabira T: Transgenic mice with Alzheimer presenilin 1 mutations show accelerated neurodegeneration without amyloid plaque formation. Nat Med 1999, 5:560–564
79. Bondolfi L, Calhoun M, Ermini F, Kuhn HG, Wiederhold KH, Walker L, Staufenbiel M, Jucker M: Amyloid-associated neuron loss and gliogenesis in the neocortex of amyloid precursor protein transgenic mice. J Neurosci 2002, 22:515–522
80. Charriaut-Marlangue C, Ben-Ari Y: A cautionary note on the use of the TUNEL stain to determine apoptosis. Neuroreport 1995, 7:61–64
81. Grasl-Kraupp B, Ruttkay-Nedecky B, Koudelka H, Bukowska K, Bursch W, Schulte-Hermann R: In situ detection of fragmented DNA (TUNEL assay) fails to discriminate among apoptosis, necrosis, and autolytic cell death: a cautionary note. Hepatology 1995, 21:1465–1468
82. Yu ZX, Li SH, Evans J, Pillarisetti A, Li H, Li XJ: Mutant huntingtin causes context-dependent neurodegeneration in mice with Huntington's disease. J Neurosci 2003, 23:2193–2202
83. Petrasch-Parwez E, Nguyen HP, Lobbecke-Schumacher M, Habbes HW, Wieczorek S, Riess O, Andres KH, Dermietzel R, Von HS: Cellular and subcellular localization of Huntingtin aggregates in the brain of a rat transgenic for Huntington disease. J Comp Neurol 2007, 501:716–730
84. Bursch W, Ellinger A, Gerner C, Frohwein U, Schulte-Hermann R: Programmed cell death (PCD). Apoptosis, autophagic PCD, or others? Ann NY Acad Sci 2000, 926:1–12
85. Gozuacik D, Kimchi A: Autophagy and cell death. Curr Top Dev Biol 2007, 78:217–245
86. Lockshin RA, Zakeri Z: Apoptosis, autophagy, and more. Int J Biochem Cell Biol 2004, 36:2405–2419
87. Krantic S, Mechawar N, Reix S, Quirion R: Molecular basis of programmed cell death involved in neurodegeneration. Trends Neurosci 2005, 28:670–676
88. Bredesen DE, Rao RV, Mehlen P: Cell death in the nervous system. Nature 2006, 443:796–802
89. Cataldo AM, Barnett JL, Berman SA, Li J, Quarless S, Bursztajn S, Lippa C, Nixon RA: Gene expression and cellular content of cathepsin D in Alzheimer's disease brain: evidence for early up-regulation of the endosomal-lysosomal system. Neuron 1995, 14:671–680
90. Nixon RA: Autophagy, amyloidogenesis and Alzheimer disease. J Cell Sci 2007, 120:4081–4091
91. Masliah E, Sisk A, Mallory M, Mucke L, Schenk D, Games D: Comparison of neurodegenerative pathology in transgenic mice overexpressing V717F beta-amyloid precursor protein and Alzheimer's disease. J Neurosci 1996, 16:5795–5811
92. Boland B, Nixon RA: Neuronal macroautophagy: from development to degeneration. Mol Aspects Med 2006, 27:503–519
93. Okamoto K, Hirai S, Iizuka T, Yanagisawa T, Watanabe M: Reexamination of granulovacuolar degeneration. Acta Neuropathol (Berl) 1991, 82:340–345
94. Selznick LA, Holtzman DM, Han BH, Gokden M, Srinivasan AN, Johnson EM Jr, Roth KA: In situ immunodetection of neuronal caspase-3 activation in Alzheimer disease. J Neuropathol Exp Neurol 1999, 58:1020–1026
95. Yoshimori T: Autophagy: paying Charon's toll. Cell 2007, 128:833–836
96. Levine B: Cell biology: autophagy and cancer. Nature 2007, 446:745–747
97. Maiuri MC, Zalckvar E, Kimchi A, Kroemer G: Self-eating and self-killing: crosstalk between autophagy and apoptosis. Nat Rev Mol Cell Biol 2007, 8:741–752
98. Xue L, Fletcher GC, Tolkovsky AM: Autophagy is activated by apoptotic signalling in sympathetic neurons: an alternative mechanism of death execution. Mol Cell Neurosci 1999, 14:180–198
99. Pattingre S, Tassa A, Qu X, Garuti R, Liang XH, Mizushima N, Packer M, Schneider MD, Levine B: Bcl-2 antiapoptotic proteins inhibit Beclin 1-dependent autophagy. Cell 2005, 122:927–939
100. Moretti L, Cha YI, Niermann KJ, Lu B: Switch between apoptosis and autophagy: radiation-induced endoplasmic reticulum stress? Cell Cycle 2007, 6:793–798
101. Bauvy C, Gane P, Arico S, Codogno P, Ogier-Denis E: Autophagy delays sulindac sulfide-induced apoptosis in the human intestinal colon cancer cell line HT-29. Exp Cell Res 2001, 268:139–149
102. Boya P, Gonzalez-Polo RA, Casares N, Perfettini JL, Dessen P, Larochette N, Metivier D, Meley D, Souquere S, Yoshimori T, Pierron

G, Codogno P, Kroemer G: Inhibition of macroautophagy triggers apoptosis. Mol Cell Biol 2005, 25:1025–1040
103. González-Polo RA, Boya P, Pauleau AL, Jalil A, Larochette N, Souquere S, Eskelinen EL, Pierron G, Saftig P, Kroemer G: The apoptosis/autophagy paradox: autophagic vacuolization before apoptotic death. J Cell Sci 2005, 118:3091–3102
104. Pyo JO, Jang MH, Kwon YK, Lee HJ, Jun JI, Woo HN, Cho DH, Choi B, Lee H, Kim JH, Mizushima N, Oshumi Y, Jung YK: Essential roles of Atg5 and FADD in autophagic cell death: dissection of autophagic cell death into vacuole formation and cell death. J Biol Chem 2005, 280:20722–20729
105. Yousefi S, Perozzo R, Schmid I, Ziemiecki A, Schaffner T, Scapozza L, Brunner T, Simon HU: Calpain-mediated cleavage of Atg5 switches autophagy to apoptosis. Nat Cell Biol 2006, 8:1124–1132
106. Espert L, Denizot M, Grimaldi M, Robert-Hebmann V, Gay B, Varbanov M, Codogno P, Biard-Piechaczyk M: Autophagy is involved in T cell death after binding of HIV-1 envelope proteins to CXCR4. J Clin Invest 2006, 116:2161–2172
107. Scott RC, Juhasz G, Neufeld TP: Direct induction of autophagy by Atg1 inhibits cell growth and induces apoptotic cell death. Curr Biol 2007, 17:1–11
108. Paxinos G, Franklin KBJ: The mouse brain in stereotaxic coordinates, 2nd Edition. London, UK Academic Press, 2001, Figure 33